Bulletin of the Seismological Society of America, Vol. 75, No. 2, pp. 519–541, April 1985

THE TWO-DIMENSIONAL RESONANCE OF SEDIMENT-FILLED VALLEYS

By Pierre-Yves Bard and Michel Bouchon

Abstract

This paper presents a numerical study of the response of relatively embanked sediment-filled valleys to incident plane *SH*, *SV*, and *P* waves, in the two-dimensional case. The Aki-Larner technique used here is shown to be reliable even for steep interface slopes. Numerical results show the existence and the importance in such valleys of specific two-dimensional resonance patterns, which may be classified in three categories: the antiplane shear modes, corresponding to *SH* motion; the in-plane shear modes (*SV*); and the in-plane bulk modes (*P*). Each of them is characterized by the consistency of the peak frequencies, and the in-phase motion (modulo 180°) across the whole valley. They induce a very large amplification, even in the case of significant damping (up to 4 times the corresponding one-dimensional prediction), a very long duration of motion, and large differential motion. The characteristics of the fundamental modes are in good qualitative agreement with the relevant experimental observations. The existence of this two-dimensional resonance is controlled by the shape ratio (thickness to half-width ratio) and the velocity contrast: a quantitative relationship is proposed in the *SH* case. The frequency of these resonance modes, for each pattern, is shown to depend only on two parameters: the one-dimensional resonance frequency at the valley center and the shape ratio. A simple model of a soft rectangular inclusion is shown to provide satisfactory quantitative formulas to estimate the fundamental resonance frequencies of any valley. As to the amplitude of this two-dimensional resonance, the general trends of its dependence on the different valley parameters (shape ratio, velocity contrast, Poisson ratio, damping) and on the incident wave field characteristics (wave type, incidence angle) are indicated. An important result, however, for earthquake engineering purposes is that both the two-dimensional resonant frequencies and amplification values differ a lot from their "classical" one-dimensional estimates.

Introduction

In two previous papers (Bard and Bouchon, 1980a, b), which will be referred to as I and II in the following, we investigated the response of relatively shallow sediment-filled valleys to incoming plane *SH* (I), *SV*, and *P* (II) waves. It was shown that the nonplanar interface causes surface waves to be generated on the valley edges and to propagate back and forth within the sediment cover. The resulting effects of engineering interest are a large enhancement of the sediment amplification, the prolongation of signal duration and the development of significant differential motion.

Some recent experimental and theoretical results lead us to extend these previous studies to deeper valleys. The most interesting and complete observations were made by Tucker and King (1984) and King and Tucker (1984). These authors instrumented three roughly two-dimensional valleys in the Garm (Tadjikistan, USSR) region, having a shape ratio between 0.2 and 0.3 (we define the "shape ratio" as the ratio of the maximum sediment thickness to the valley half-width l). As detailed in their papers, these rather deep valleys exhibit specific resonance patterns, whose characteristics are the following.

1. The frequency of the gravest peak is the same at each site within the valley, regardless of local sediment thickness.

2. The corresponding amplification is the largest in the valley center, and decays toward the edges, where it vanishes.
3. At this frequency, the ground motion is in phase across the whole valley (Bard and Tucker, in preparation, 1985).

On a much different scale, observations (1) and (2) stand also for the long period (T = 1 to 5 sec) microtremor noise measurements of Kagami *et al.* (1982) on the two sites of Niigata and San Fernando. In both areas, the thickness of sedimentary deposits varies from 6 to 8 km to 0 km over only a few tens of kilometers (which gives similar shape ratio values).

These experimental results are to be compared with the sparce theoretical work concerning the seismic response of embanked sedimentary deposits. Trifunac (1971), Wong and Trifunac (1974), Sanchez-Sesma and Esquivel (1979) investigated the antiplane (SH) response of very deep semi-elliptical, sine-shaped or triangle-shaped valleys at single frequencies, and found very large amplifications at unexpected frequencies. Trifunac (1971) showed that the transfer functions for different sites at the surface of a semi-circular valley exhibit identical resonance frequencies [feature (1)], and we noticed in II an in-phase large amplitude motion for the deepest ($h/l = 0.2$) sine-shaped valley considered [feature (3)].

These are converging indications suggesting the existence in embanked sedimentary deposits of specific resonance patterns. The aim of the present paper is to achieve a better understanding of the nature and main characteristics of this phenomenon. This will be done by means of a numerical study of the elastic response of two-dimensional deep soft structures embedded in a harder half-space to incoming plane waves, in both cases of in-plane motion (P and SV waves) and antiplane motion (SH waves).

The Numerical Method

The numerical method used for this study is still the Aki-Larner technique. It has been described with much detail by Larner (1970) and Aki and Larner (1970), and its theoretical reliability for its present application to sediment-filled valleys has been carefully discussed in I and II.

The applicability of the method to deep valleys with relatively steep sediment-basement interface is demonstrated in Figure 1 where a comparison with the collocation method of Sanchez-Sesma and Esquivel (1979), whose accuracy has been carefully tested by the authors, is presented. The shape ratio h/l considered is a large as 1.2, which corresponds to a maximum interface slope of 63°. The discrepancy between both sets of results is never larger than 15 per cent, which is certainly below the error induced by modeling the sediments rheology with the "ideal" linear homogeneous isotropic elasticity.

In spite of these successful tests for very deep valleys, we have limited our present study to valleys having a shape ratio lower that 0.8, and a higher sediment-basement impedance contrast (between 5 and 8, against 3 in Figure 1). Therefore, from the discussion of Bard (1983), we may expect that the maximum inaccuracy of the present results lies well below 10 per cent.

Theoretical Evidence for Specific Resonance Patterns in Deep Valleys

SH case

The difference between the theoretical results for shallow valleys (I, II) and the experimental data for deep valleys (Kagami *et al.*, 1982; Tucker and King, 1984;

King and Tucker, 1984) strongly suggests that two-dimensional resonance only occurs in relatively embanked sediment-filled valleys.

Figure 2 shows the influence of the shape ratio h/l on the antiplane (SH) Fourier transfer functions for several points located at the surface of a sine-shaped valley. The density and velocity contrast values choosen are large but not unrealistic (e.g., Tucker and King, 1984). Damping is not considered in this case, so as to better see the valley behavior.

The most striking feature concerns the amplitude of the gravest peak. For any given location, it strongly depends on the shape ratio. The largest values occur for $h/l = 0.4$. The amplification at the valley center is then much larger (about 3.5 times) than the impedance contrast, which represents the one-dimensional amplification value. Moreover, the frequency f_0 of this gravest peak, which is very near

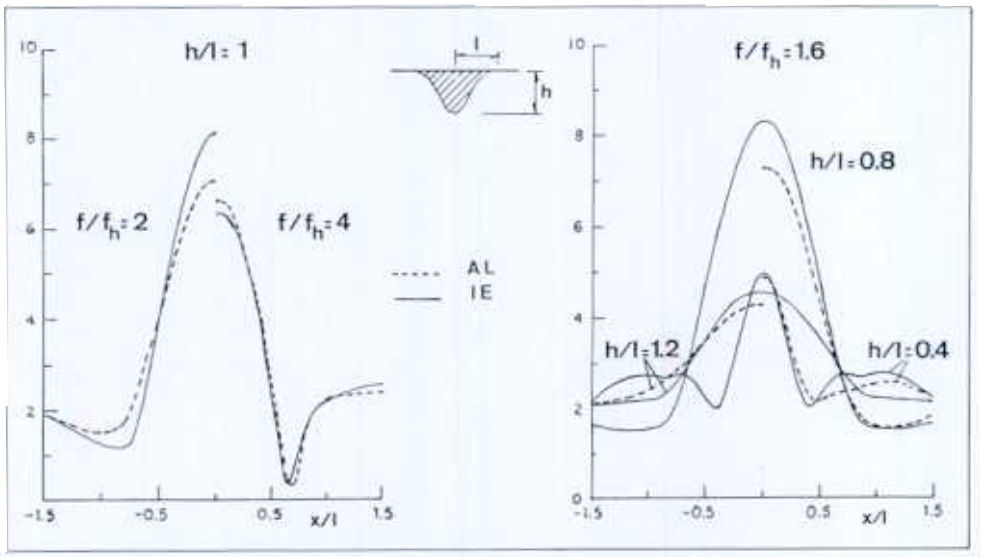

FIG. 1. Comparison between the Aki-Larner technique (AL) and the integral equation method (IE) of Sanchez-Sesma and Esquivel (1979). The shape of the valleys considered is depicted on *top*. The velocity and density contrasts are, respectively, 2 and 1.5. The incoming waves are vertical SH waves. fh is the one-dimensional resonance frequency at the valley center, $fh = \beta_1/4h$. The curves represent the amplitude of surface motion as a function of the dimensionless abscissa x/l. (*Left*) Response of one valley ($h/l = 1$) at two different dimensionless frequencies: $f/fh = 2$ and $f/fh = 4$. (*Right*) Response of three different valleys ($h/l = 0.4$, 0.8, and 1.2) at one dimensionless frequency $f/fh = 1.6$.

the one-dimensional resonance frequency $f_h = \beta 1/4h$ for the shallowest valley ($h/l = 0.2$), becomes significantly larger for deeper valleys: $f_0 = 1.31\, f_h$ for $h/l = 0.4$, and $f_0 = 1.76\, f_h$ for $h/l = 0.8$.

The time domain behavior corresponding to Figure 2 ($h/l = 0.2$) has been illustrated in Figure 7 of I. The prominent feature was shown to be the development of Love waves within the sediment cover and their subsequent back and forth propagation across the valley.

The time domain behavior corresponding to Figure 2 ($h/l = 0.4$) is illustrated in Figure 3. The incident signals, displayed at the bottom of this figure, have been taken as transient but quasi-monochromatic wavelets having respective characteristic frequencies equal to that of the first two peaks: $f_0 = 1.31\, fh$ and $f_1 = 2.33\, fh$. Figure 3 shows very clearly that we are dealing with resonance patterns involving the valley as a whole, the characteristics of which are the following.

1. The fundamental mode ($f = f_0 = 1.31\ fh$, Figure 3, left) concerns mainly the central part of the valley, although the resonance is observable up to $x/l = 0.6$. The motion is in phase across the whole valley. Its amplitude is very large, and decreases regularly from the center to the edges: the peak value is 8 times larger at the center than at the edges or on the bedrock. The duration of shaking is very long: in the present case of zero damping, the amplitude at the valley center after 10 cycles is still 6 times larger than the peak value at the signal onset on the edges. It must be said again that the frequency is significantly different from the one-dimensional resonance frequency $f_0/fh = 1.31$.
2. The first higher mode ($f = f_1 = 2.3\ fh$, Figure 3, right) displays displacement nodes at $x/l = \pm 0.16$. There are therefore, spatially, three amplitude maxima:

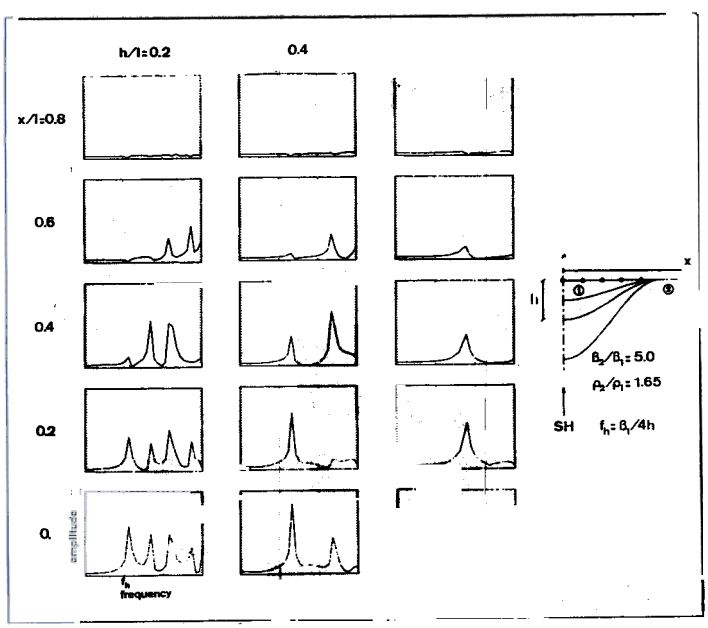

FIG. 2. Effects of the shape ratio on the response of a high-contrast sine-shaped valley to vertical *SH* waves. The curves represent the spectral transfer functions for five surface sites, regularly spaced from the center (*bottom row*) to the edge (*top row*). Three different shape ratios are considered; the shallowest valley is at the *left* and the deepest is at the *right*. The frequency range is [0, 3 *fh*], and the amplitude scale is given at the *bottom left*. Valley characteristics and site location are detailed on the *right*.

one at the valley center (because of symmetry) and the other two at $x/l = \pm 0.4$. The motion is in phase between two adjacent nodes, and changes sign at each node. Like for the fundamental mode, the amplification is large: 3.7 at the valley center and 5.0 at mid-edge. This first higher mode, observable up to $x/l = 0.7$, affects a wider part of the valley than the fundamental mode. Its frequency $f_1 = 2.3\ fh$ bears no relation to the one-dimensional harmonic frequencies $f_n' = (2n + 1)\ fh$.

Looking at the depth dependence of ground motion amplitude and phase also provides a valuable insight into the nature and origin of these specific resonance patterns. For instance, in the one-dimensional case, the plane layer resonance modes display a sinusoidal dependence, with a maximum at the surface, a node at the interface, and a number of intermediate nodes equal to the order of the harmonics.

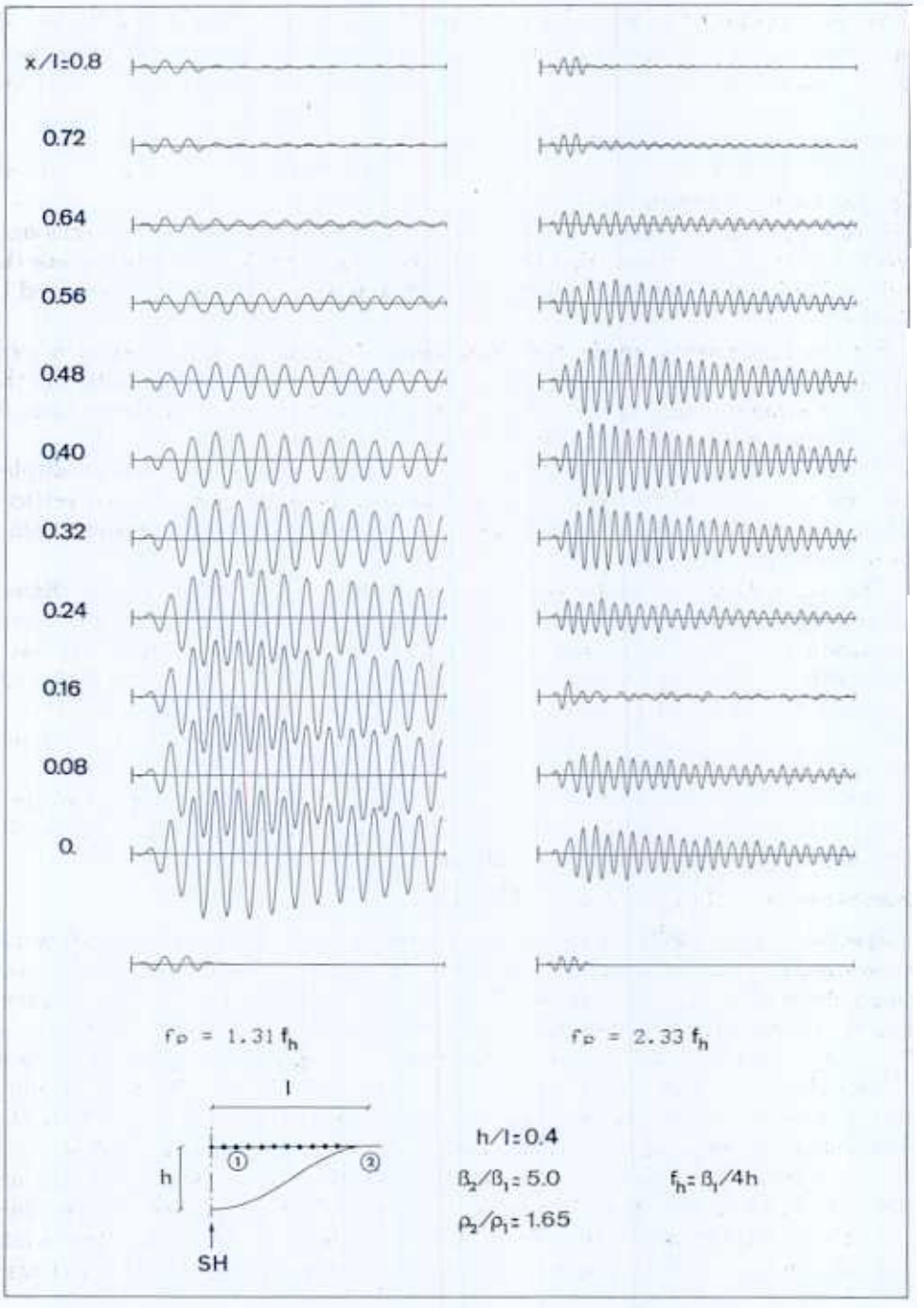

FIG. 3. Time domain illustration of the first two *SH* resonance modes of a sine-shaped valley. Each column of seismograms represents the surface motion at 11 surface sites, regularly spaced from the center ($x/l = 0$, *bottom*) to the edge ($x/l = 0.8$, *top*), when the valley is impinged by the incident signal displayed at the *bottom*. On the *left* is the fundamental mode ($fp = 1.31\ fh$) and on the right the first higher mode ($fp = 2.33\ fh$). The amplitude scale is the same in both cases: the vertical bar on the *left* of each seismogram corresponds to an amplification range $[-1, +1]$. The valley characteristics are detailed on the *bottom*, and the time window is $10.67/fh$.

Figure 4 displays this depth dependence of ground motion for the first five modes of the sine-shaped valley already investigated in Figures 2 and 3. These figures have been obtained by exciting the valley at the resonance frequencies with transient signals similar to those shown in Figure 3, and then "taking a picture" of the ground motion on a valley cross-section at equally spaced times. The time step is, in each case, one-eighth of the corresponding mode period, so that three snapshots represent one-fourth of a complete cycle.

A common and striking feature is that for each mode the motion concerns only the sediments, which means that the energy is almost completely trapped inside the valley. This explains both the huge amplifications and long durations observed in Figure 3.

For the fundamental mode, the depth dependence at the valley center is very similar to that of a resonant plane layer. However the amplitude distribution in the x-z plane strongly suggests that this fundamental mode results from the focusing of incoming waves toward the valley center.

Contrary to plane layer harmonics, the first higher mode ($f = f_1$) does not display any node at intermediate depth. On the opposite, its nodal line is almost vertical, which is a good indication that this particular resonance mechanism results mainly from lateral interferences.

The higher harmonic patterns become more and more complex and are characterized by the presence of an increasing number of lateral nodes as their order increases: this shows once again the importance of lateral interferences. Also noticeable however are the nodes at intermediate depth for the modes 2 (1 node around $x/l = 0.15$) and 4 (2 nodes at $x/l = 0$). Their presence is to be related with the fact that the respective frequencies of these two modes do not differ too much from the one-dimensional harmonics $f_1' = 3\,fh$ and $f_2' = 5\,fh$.

The main conclusion of these observations is that these two-dimensional resonance patterns involve both vertical and lateral interferences, which explains why they appear only in relatively deep valleys.

Plane strain case: incident P and SV waves

Spectral studies similar to the one illustrated in Figure 2 (see Bard, 1983) would show that, for incident P and SV waves too, the spectral peaks become particularly sharp above some particular values of the shape ratio h/l. For a sine-shaped valley having the same elastic parameters as those of Figures 2 to 4, and Poisson ratio of 0.33 in the sediments and 0.25 in the bedrock, this particular shape ratio has been found to be $h/l = 0.3$ in the SV case, and $h/l = 0.6$ in the P case. The corresponding resonant frequencies are respectively: $f_0(SV) = 1.41\ \beta_1/4h$, and $f_0(P) = 1.16\ \alpha_1/4h$, which are once again significantly different from the one-dimensional values.

The time domain behaviors corresponding to these sharp spectral peaks are shown in Figure 5. The presentation is the same as in Figure 3, except that there are now two components of motion. The characteristics of these plane strain resonance patterns are qualitatively very similar to those observed in the SH case, with nevertheless some slight differences.

1. In both cases, the motion is strongly amplified in the central part of the valley, and this amplification gradually decays toward the edges, where it vanishes. In the present case of a strong impedance contrast, the amplification reaches a value of 8 at the valley center for the main component, while the other component is maximum around $x/l = 0.2$ to 0.4, where it is approximately twice the maximum motion on bedrock. These resonances extend up to $x/l = 0.7$ in the SV case, and up to $x/l = 0.5$ in the P case.

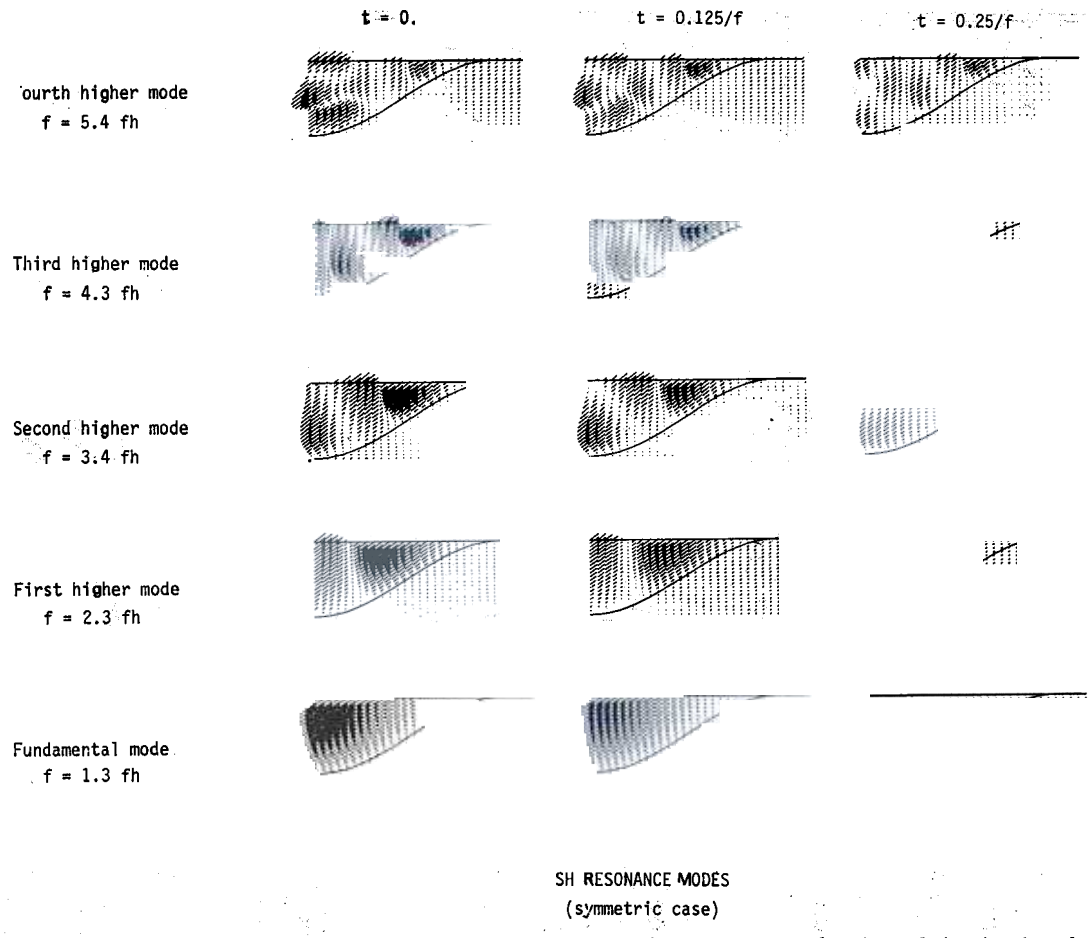

FIG. 4. Variations of ground motion amplitude on a valley cross-section for the first five *SH* resonance modes. At each (x, z) point, the amplitude of the antiplane motion is given by the length of the oblique segment. The valley characteristics are the same as in Figure 3. The incoming waves are vertical *SH* waves. See text for further details.

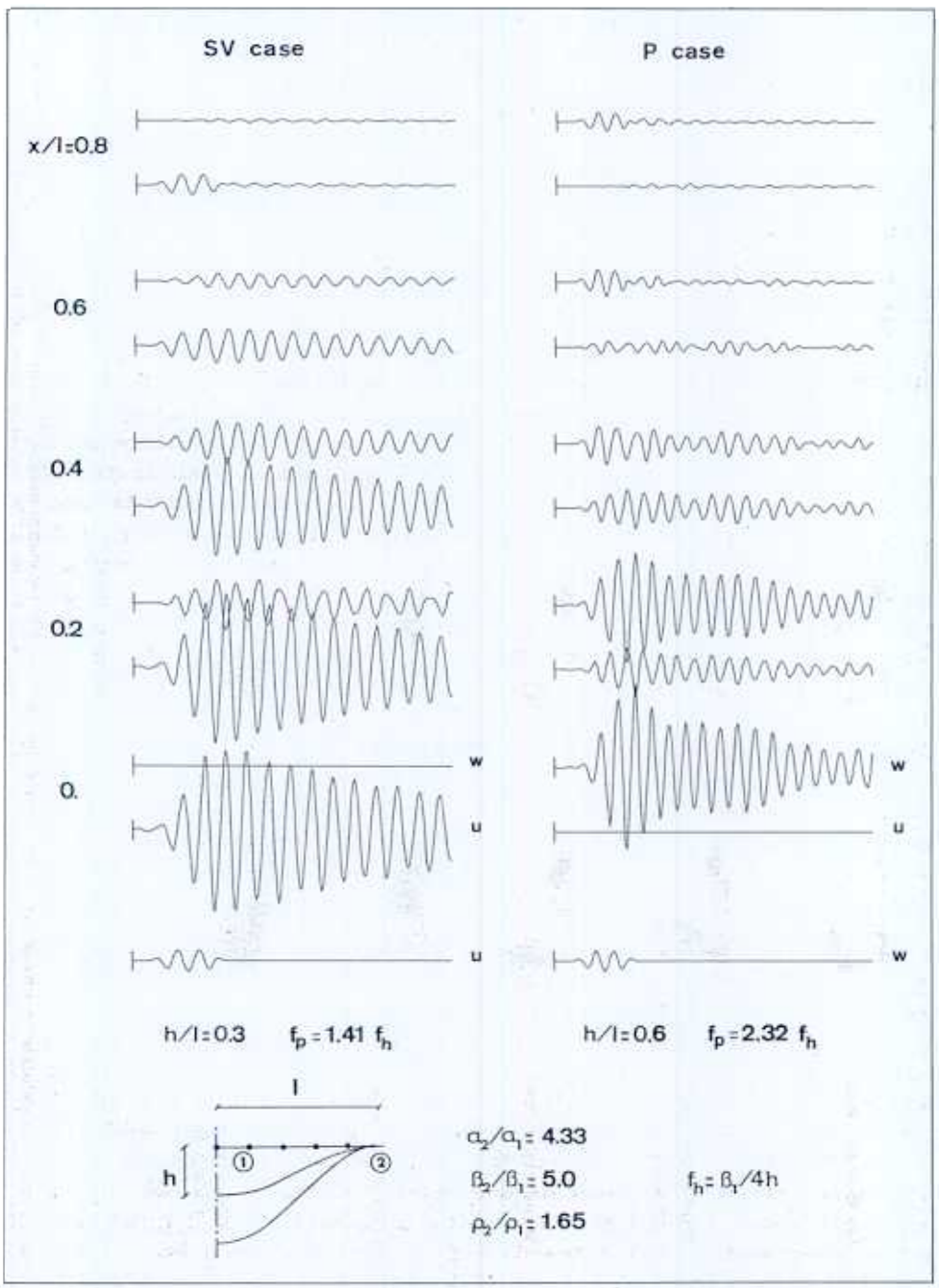

FIG. 5. Time domain illustration of the fundamental modes of a sine-shaped valley in the *SV* (*left*) and *P* (*right*) cases. The geometry and the mechanical parameters of the valley are detailed on the *bottom*, together with the characteristic frequency *fp* of the incoming signal. Each set of two seismograms represent the in-plane horizontal motion (*bottom trace*, *u*) and vertical motion (*top trace*, *w*). A positive *u* corresponds to a motion towards the right, and a positive *w* to a downward motion. Each surface site selected is characterized by its dimensionless abscissa *x*/*l*, measured from the valley center. The amplitude scale is the same in both cases and is given in the same way as in Figure 3.

2. The motion duration is very long in both cases. The amplitude decay with time is roughly the same as in the *SH* case.
3. The phase of the main component of motion (i.e., horizontal in the *SV* case and vertical in the *P* case) is the same across the whole valley, while the other component changes sign at the center. Moreover, at each site, the two components have the same phase modulo 180°. The *SV* resonance is an in-plane shearing pattern and may be thought of as a rocking of the whole valley around its central axis. The *P* resonance, on the other hand, is a succession of expansions and contractions, and may be visualized as a "respiration" of the valley (Figure 6).

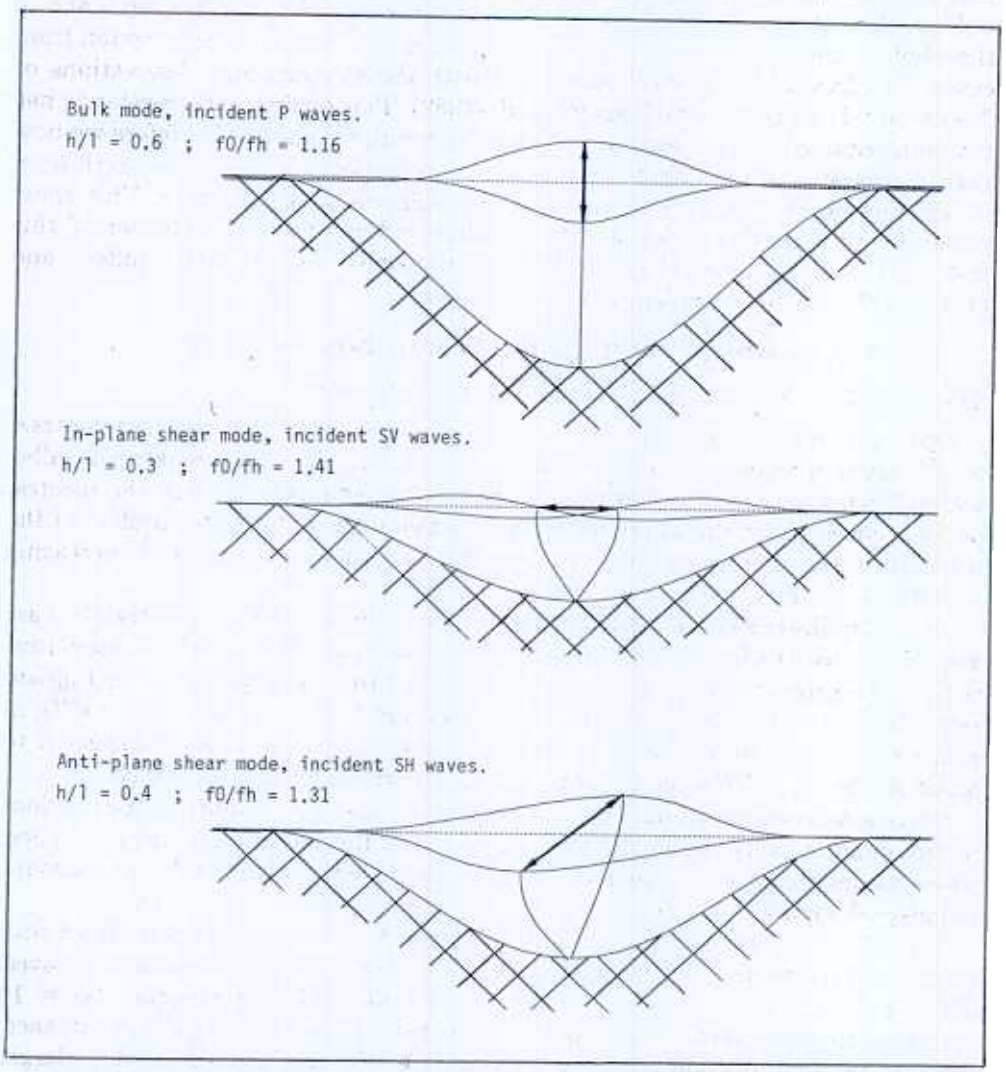

FIG. 6. Illustration of the three fundamental modes of a sine-shaped valley: antiplane shear mode (*bottom*), in-plane shear mode (*middle*), and in-plane bulk mode (*top*). Each of them has been represented for the corresponding critical shape ratio. The antiplane motion (*SH* case) has been plotted along an oblique axis. For each mode, we have displayed the distribution of motion along the surface and along a vertical line at the valley center, at the two times of maximum motion: t_0 and $t_0 + 0.5/f_0$. The dotted line is the free surface at rest and also at the time $t_0 + 0.25/f_0$.

Conclusions

Numerical results show the existence in relatively deep two-dimensional sediment-filled valleys of specific two-dimensional resonance patterns, which may be classified in three categories as illustrated in Figure 6: the antiplane shear modes (SH), the in-plane shear modes (SV), and the in-plane "bulk" modes (P).

Their three main characteristics, i.e., the consistancy of the peak frequency across the whole valley, the in-phase motion, and the gradual decay of amplification from center to edges, are in perfect agreement with the experimental observations of Tucker and King (1984) and Kagami *et al.* (1982). This qualitative consistancy has yet been obtained, in this section, only on a particular example. Therefore we now need to investigate the effects of the valley properties and of seismic excitation parameters on the characteristics of this two-dimensional resonance. This short parameter study will provide a better understanding of the mechanism of this resonance, of its link with the lateral propagations observed in shallow valleys, and of the conditions under which resonance occurs.

Sensitivity Study and Physical Interpretation

Effect of valley properties and seismic excitation parameters

Effect of impedance contrast and Poisson ratio. The effect of impedance contrast is illustrated in Figure 7a. The configuration considered is still a sine-shaped valley with $h/l = 0.4$ impinged by vertical SH waves. The main result is that the spectral peaks occur at about the same frequencies (scaled to $fh = \beta_1/4h$), regardless of the impedance contrast. As expected, the amplification values increase with increasing impedance contrast.

Figure 7b illustrates the effects of the sediment Poisson ratio ν_1 in the SV case and shows that the fundamental frequency, still scaled to $fh = \beta_1/4h$, is insensitive to this parameter. The corresponding spectral amplitude yet depends on the Poisson ratio, but in a rather irregular way: the largest amplification occurs for $\nu_1 = 0.33$, in which case the P velocity contrast is equal to 4.33, while one would expect it to occur for the largest P velocity contrast, i.e., 5, corresponding to $\nu_1 = 0.25$.

Effect of sediment damping. The very large amplifications obtained in the previous figures point out very clearly the phenomenology of the two-dimensional resonance. These values are, however, somewhat unrealistic since they do not take into account sediment damping.

The effect of damping is analyzed in Figure 8. The example considered still involves a high contrast sine-shaped valley ($h/l = 0.4$) excited by vertical SH waves. The amplification is strongly reduced in case of a high attenuation ($Q = 10$ corresponding to a damping of 5 per cent), but it still remains large. For instance, the spectral amplification at the valley center for the fundamental mode is larger for a Q of 10 (about 10) than the one-dimensional amplification value without attenuation (8.25).

It is to be noted also that, as for all resonance phenomena, the damping reduces much more the amplitude of the harmonics than that of the fundamental.

In the time domain, the sediments damping acts more on signal duration than on maximum amplitude: Figure 8 shows that, between $Q = \infty$ and $Q = 10$, the motion amplitude is reduced by less than 30 per cent, while the number of cycles is reduced by a factor of about 3. This observation leads us to remark, incidentally, that it is probably much easier and more reliable to measure damping in soils with the coda decay than with the amplitudes of first arrivals.

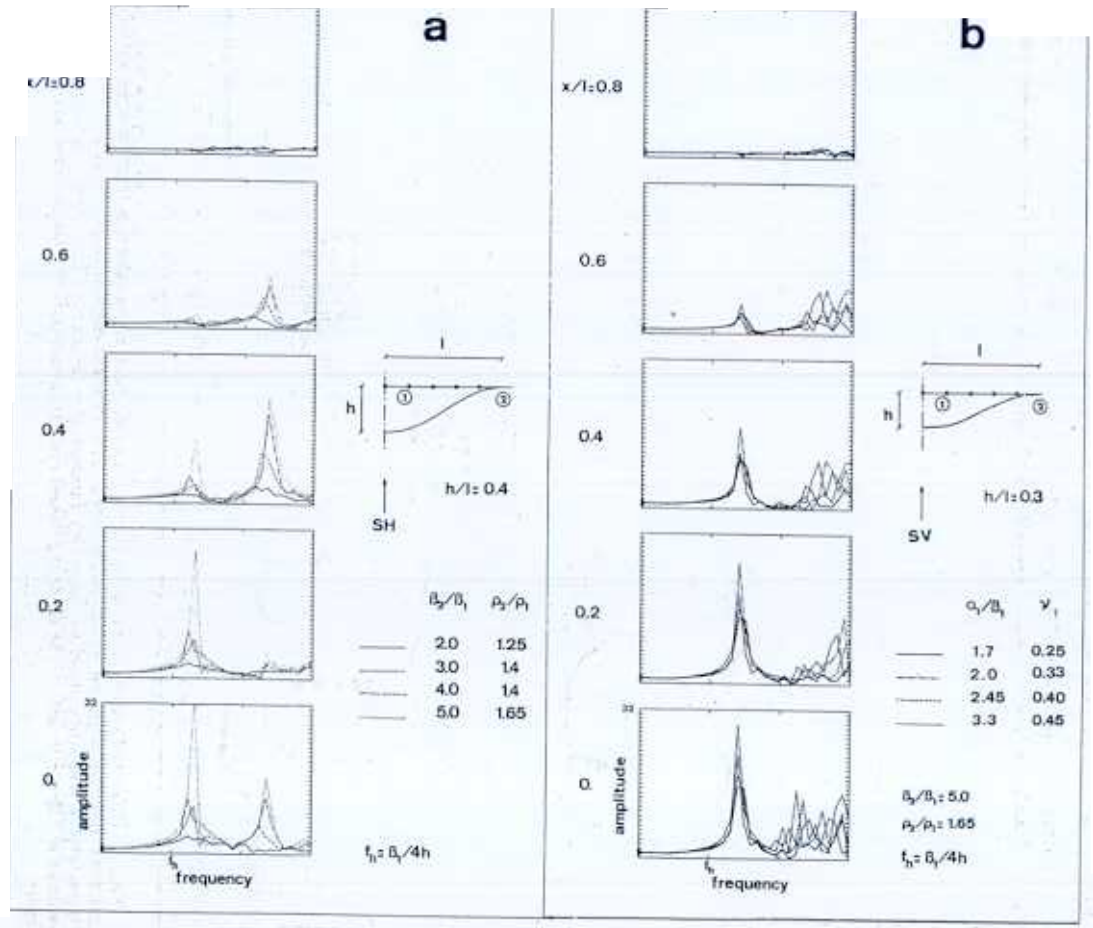

FIG. 7. Effects of impedance contrast [*left*, *SH* case (a)] and Poisson ratio [*right*, *SV* case (b)]. In both cases are plotted the spectral transfer functions for the adequate horizontal component, at several surface sites. The frequency and amplitude scales are given on the *bottom left*. The valley geometry and mechanical parameters are detailed at the *right* in both cases.

Effect of incidence angle. When the waves are obliquely incident, as in Figure 9 (*SH* case), the problem configuration is no longer symmetric. We, therefore, observe antisymmetric resonance modes at intermediate frequencies, characterized by a displacement node at the valley center and maxima at mid-edges. Figure 9 also shows, however, that the frequencies of each mode, either symmetric or antisymmetric, are not affected at all by the value of the incidence angle.

Figure 9 clearly shows, too, that the amplitude of the symmetric modes is

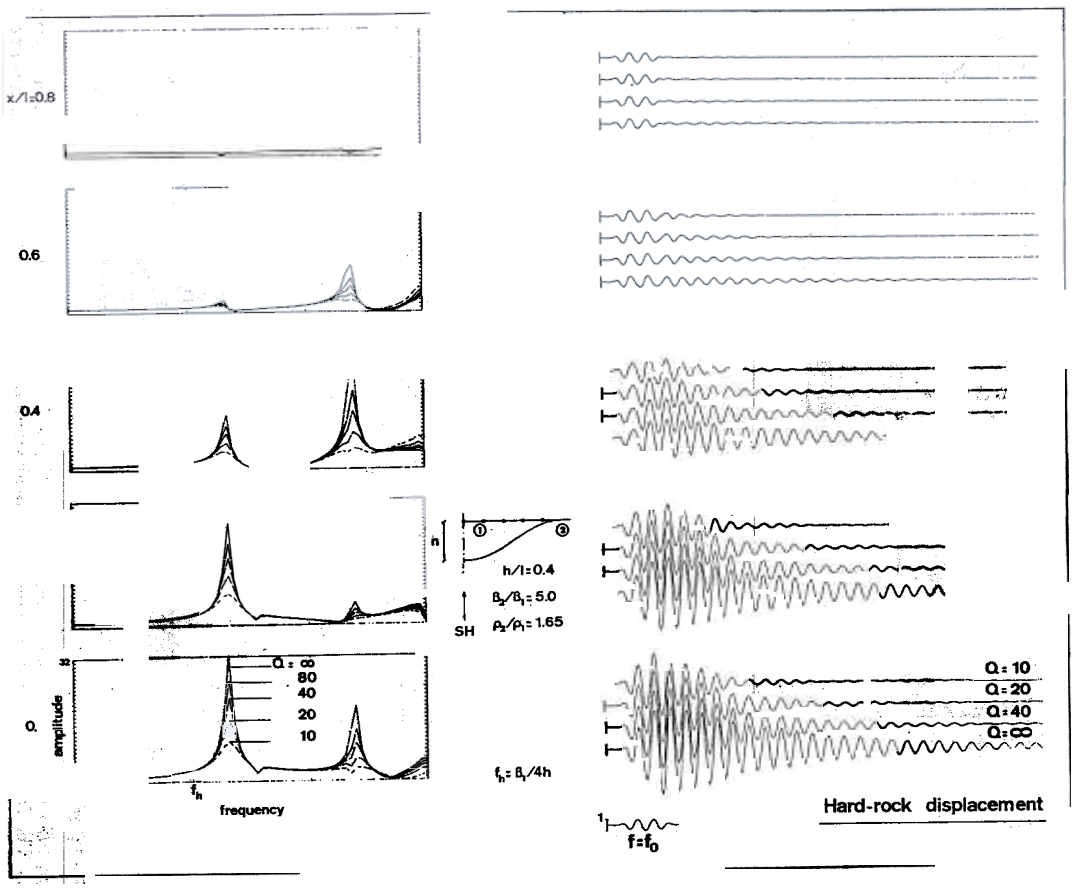

FIG. 8. Effects of sediment damping in the *SH* case: spectral transfer functions at some surface sites and time domain response at the same sites. The incident signal, displayed on the *bottom*, has a characteristic frequency equal to the valley fundamental frequency. The valley characteristics are the same as in Figures 3 and 4. The damping values and frequency and amplitude scales are detailed in the figure.

maximum in the case of vertical incidence and is significantly reduced for oblique waves. It may be noticed, however, that the amplification values stay about the same when the incidence angle changes from 30° to 60°. Another interesting feature is that, at least for the gravest symmetric and antisymmetric modes, there is no significant difference between the two sides of the valley for all the incidence angles considered: this is related to the fact that we are dealing with global resonance modes, involving the whole valley.

Link with the behavior of shallow valleys

It has been shown (I, II, and Harmsen and Harding, 1981) that shallow valleys give rise to the development of surface waves which then propagate back and forth within the sediment cover. This type of behavior may also be observed in deep valleys, as illustrated in Figure 10 for the sine-shaped valley of Figures 3 and 4. When the input signal is relatively monochromatic and when its frequency f is close to that of a valley mode (Figure 10, a and c), the valley enters into resonance immediately. However, when f falls between two harmonics, as in Figure 10b, the phase of motion is regularly varying from valley edge to center, which is a good

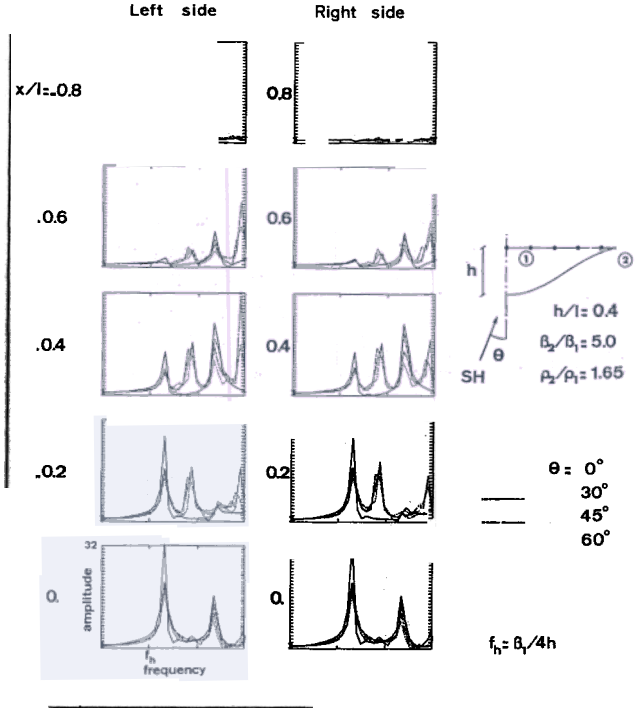

FIG. 9. Effects of incidence angle in the *SH* case. The spectral transfer functions are given for symmetric surface sites: the *left-hand side column* stands for the left side of the valley, and the valley is the same as in Figures 3, 4, and 8. The incidence angle values are given on the *right*. The frequency and amplitude scales are also given on the *bottom left* of the figure.

evidence for lateral wave propagation. It is clear yet that in the case of an incoming real earthquake signal, for which the frequency range is broad, the two-dimensional resonance pattern will dominate, since it is associated with very sharp peaks in the transfer functions of any site within the valley (see Figure 2).

The time-space behaviors shown in Figure 10, combined with the observations made in Figure 4, lead naturally to the following interpretation: "lateral waves" (easily identifiable as surface waves for shallow sediment covers, see I and II), are generated at the valley edges regardless of the shape ratio. When this shape ratio is small, this phenomenon is well separated from the vertical resonance at the valley center, since these surface waves arrive there well after the direct arrival and the

main vertical reflections. When the valley width and thickness are comparable however, the wavelength of these lateral waves is close to the valley width, which results in lateral interferences. These, in conjunction with the well-known vertical interferences, give rise to the development of specific two-dimensional resonance patterns. Finally, for the (rather unrealistic) limit case of a very deep and very narrow valley for which the width to thickness ratio would be very small (that is for some kind of sediment-filled trench), only lateral interferences would exist, resulting in one-dimensional "horizontal" resonance patterns.

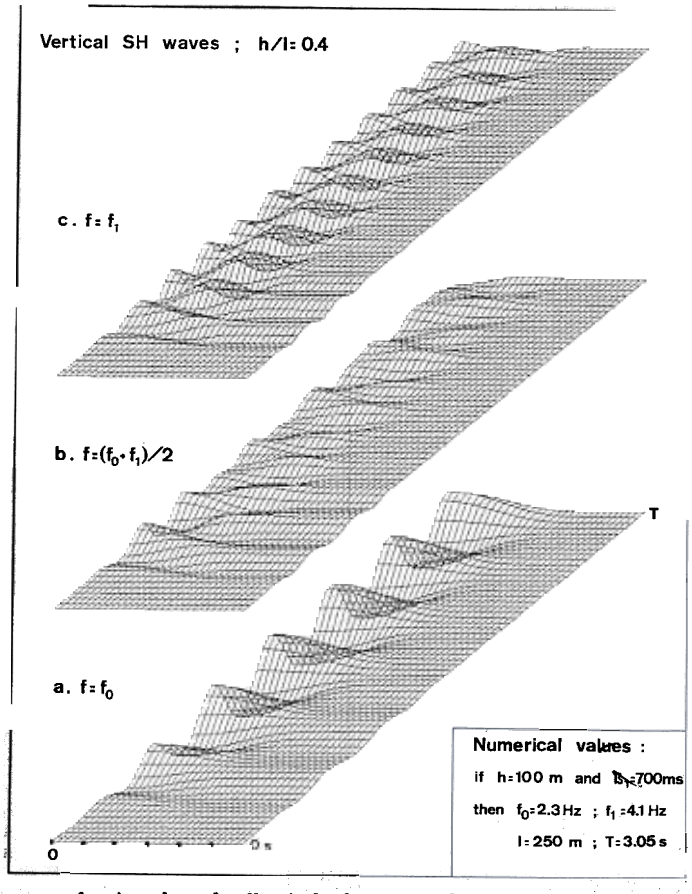

FIG. 10. Response of a sine-shaped valley in both space and time domains, to three different quasi-monochromatic *SH* signals. f_0 and f_1 are the frequencies of the gravest peaks in Figure 2 ($h/l = 0.4$). The horizontal, oblique, and vertical axis represent, respectively, the abscissa across the valley, the time, and the amplitude of antiplane motion. Only one-half of the valley is considered because of symmetry: the left part of each diagram corresponds to the valley center, and the right part to the bedrock on the edge.

Such an interpretation explains the existence of a particular shape ratio for which the amplification is maximum, as observed for $h/l = 0.4$ in Figure 2. Moreover, it is also supported by the fact that this particular shape ratio is the lowest in the *SV* cases, and the largest in the *P* case. We have shown in II that, in shallow valleys, an *SV* wave excitation induces mostly first higher mode Rayleigh waves which have a phase velocity close to the sediments *P* wave velocity (for frequencies around fh). In the case of a *P* wave excitation, on the other hand, the valley response consists mainly of fundamental Rayleigh waves, the phase velocity of which is close to the sediments shear wave velocity. The corresponding wavelengths are therefore much

larger in the former case, and the two-dimensional resonance thus occurs in shallower (or wider) valleys.

The question then arises of how the transition occurs between these two types of valley behavior. Figure 11 displays the motion phase (a) and amplitude (b) as a function of site location x/l for seven high-contrast sine-shaped valleys with increasing shape ratios (from 0.1 to 0.8). These curves correspond to vertically incident SH harmonic waves with frequency f_0. The most interesting feature in Figure 11a concerns the zone of constant phase (90°) in valley center. From very narrow for

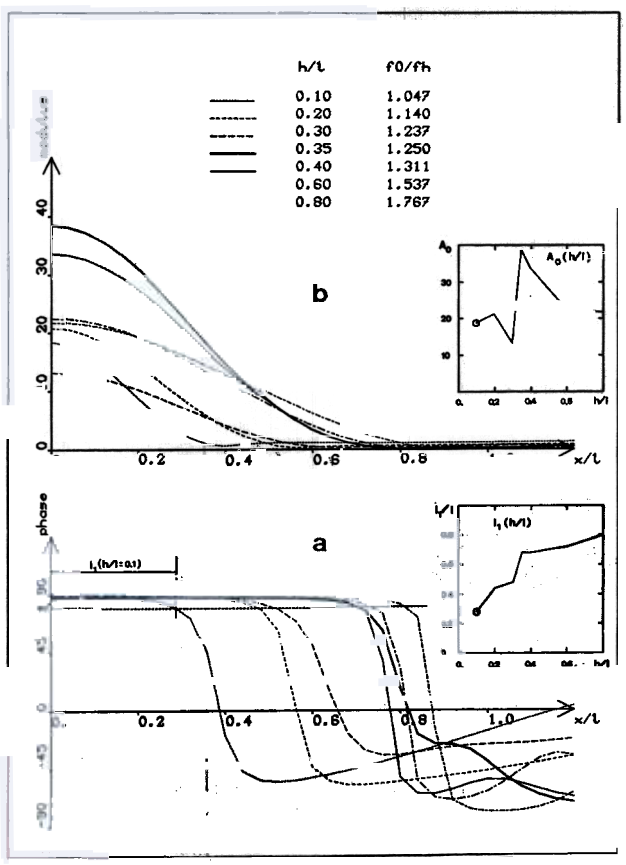

FIG. 11. Dependence of motion phase (a) and amplitude (b) on site location x/l, for seven high-contrast sine-shaped valleys with increasing shape ratios (detailed on *top*). In the small frames on the *right* are displayed the dependence on h/l of (a) the half-width l_1, scaled to the valley half-width l, over which the motion phase is larger than 80° (*bottom*), and (b) the motion amplitude A_0 ($x = 0$) at valley center. The velocity contrast, density contrast, and sediment damping are respectively 5.0, 1.65, and 0 per cent.

$h/l = 0.1$, its width regularly increases up to $h/l = 0.3$, then suddenly raises between $h/l = 0.3$ and $h/l = 0.35$, beyond which value it is almost constant around 0.7 to 0.8 l. The amplitude curves (Figure 11b) display two similar features: the amplification value at valley center exhibits a very sharp jump (from 13 to 38) between $h/l = 0.3$ and $h/l = 0.35$, such as the width of the central zone of large amplification.

These consistent observations allow us to introduce the concept of a "critical shape ratio," below which the seismic behavior of a valley is mainly characterized by one-dimensional resonance and surface wave propagation, and beyond which the main phenomenon is the two-dimensional resonance. Nevertheless, as both types

of behavior have the same physical origin, that is the deflection of incoming rays at valley edges, one must bear in mind that this concept of critical shape ratio is related much more to the sharpness of the transition between the two behaviors, than to any kind of discontinuous process.

In the present case of a high contrast sine-shaped valley impinged by *SH* waves, this critical shape ratio is clearly located between 0.3 and 0.35. As previously discussed, its value depends on the incident wave type: it falls between 0.2 and 0.3 in the *SV* case, and between 0.5 and 0.6 in the *P* case. It also depends on the valley characteristics: since the ray deflection at valley edges is controlled by the velocity contrast, one may expect the critical shape ratio to depend on this parameter. On

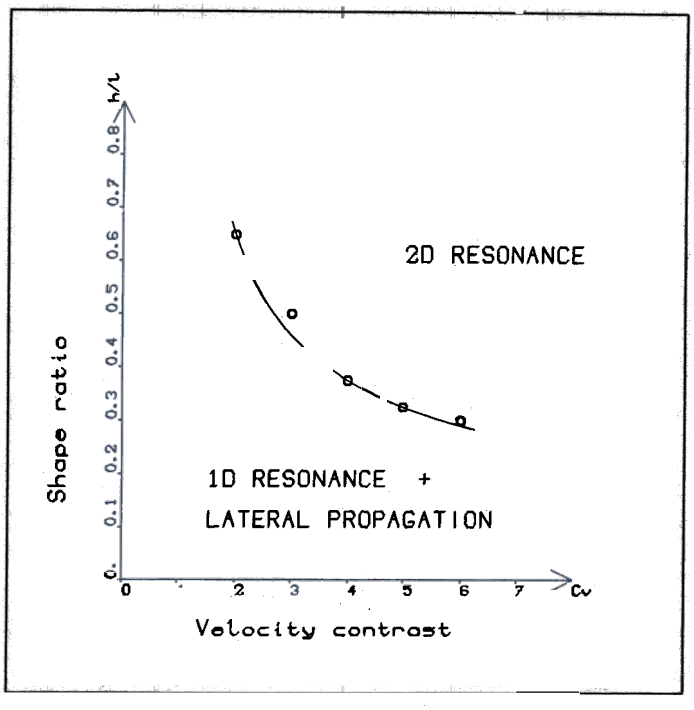

FIG. 12. Existence conditions of the two-dimensional (2D) resonance in the *SH* case. For a sine-shaped valley having a shape ratio h/l and a velocity contrast C_v, the two-dimensional resonance will exist if the corresponding point in the $(C_v, h/l)$ plane is above the delimiting curve. Below this curve, the main phenomenon is the lateral propagation of surface waves. The continuous line has been fitted on the five "experimental" points and follows the analytical formula: $(h/l)_c = 0.65/\sqrt{C_v - 1}$.

the opposite, the sediment damping acts only on the amplitude of the two-dimensional resonance and has no influence on the critical shape ratio.

The dependence of the critical shape ratio on the velocity contrast for sine-shaped valleys impinged by *SH* waves is illustrated in Figure 12, which summarizes the results of an extensive parameter study. These results confirm and quantify the intuitive expectations: the larger the velocity contrast, the lower the critical shape ratio. The curve of Figure 12 has been obtained with sine-shaped valleys only, but may be shown (Bard, 1983) to be valid also for any valley shape, provided that the real shape ratio h/l be replaced by an "equivalent" shape ratio $h/2w$ where $2w$ is the total width over which the sediment thickness is more than half its maximum value.

Resonance frequencies of a soft rectangular inclusion

Let us consider the model illustrated in Figure 13, consisting of a rectangular inclusion filled with an elastic material (density ρ_1, shear velocity β_1), embedded in a rigid half-space. The free vibrations of such an inclusion are necessarily characterized by zero displacements along the three sides bordering the rigid half-space, and zero stresses at the free surface. Furthermore, the displacement field within the elastic medium must satisfy the equation of motion.

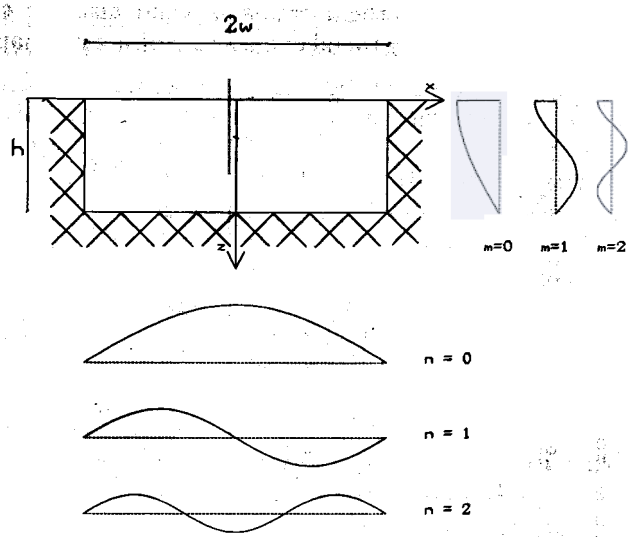

FIG. 13. Antiplane vibration modes of an elastic rectangular inclusion embedded in a rigid half-space. The curves on the *bottom* represent the admissible variations of motion amplitude along the x axis, and the curves on the right represent the admissible variations of motion amplitude along the z axis. The n and m indexes correspond to the harmonics order as explained in the text.

In the antiplane (SH) case, the displacement field has therefore the following form

$$v\ (x, z, t) = \cos(\gamma_m z) \cdot \sin(k_n(x + w)) \cdot \exp i \cdot 2\pi f t)$$

with

$$k_n = (n + 1)\pi/2w$$
$$\gamma_m = (2m + 1)\pi/2h$$
$$k_n^2 + \gamma_m^2 = 4\pi^2 f^2/\beta_1^2.$$

The resonant frequencies are, therefore

$$f^{nm} = fh\sqrt{(2m + 1)^2 + (n + 1)^2\, h^2/w^2}$$

with

$$fh = \beta_1/4h.$$

As illustrated in Figure 13, these resonance modes are associated with both vertical interferences (characterized by their order m) and lateral interferences (order n). The harmonics may be separated into two categories: the symmetric

modes ($n = 2p$), with a displacement maximum at the center, and the antisymmetric modes ($n = 2p + 1$), with a displacement node at the center.

As shown in Figure 14, this formula predicts very accurately the fundamental *SH* resonance frequencies of the sine-shaped valley provided that the equivalent width $2w$ is choosen equal to the valley half-width l. This relation can be extended to any valley shape, taking as equivalent width $2w$ the length over which the local sediment thickness is greater than half the maximum thickness (Bard, 1983). It may be shown also (Bard, 1983) that when the valley shape is not too far from a rectangle (that is with a flat central part), the formula is valid also for estimating the frequency of the first harmonics. In the above sample of a sine-shaped valley, the

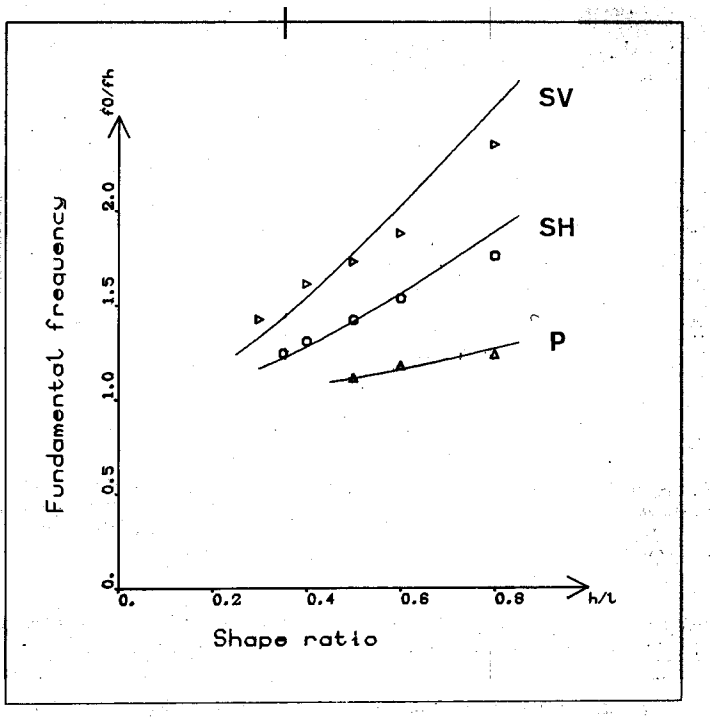

FIG. 14. Dependence of the dimensionless frequency f_0/fh on the shape ratio for the *SH*, *SV*, and *P* fundamental modes. The symbols represent the results of the Aki-Larner computations and were obtained for sine-shaped valleys having the same velocity and density contrasts as in Figures 3 and 5. The continuous lines correspond to the approximate formulas given in the text.

agreement is still relatively good, since $f_1 = 2.3\ fh$ while the predicted value is 2.6 (first higher symmetric mode: $n = 2$ and $m = 0$).

Because of the coupling between *P* and *SV* waves, the in-plane modes are more complex and, even in the simple case of a rectangular inclusion, the resonance frequencies cannot be expressed in a simple form. However, from the results displayed in Figure 14 and by analogy with the *SH* case, we obtain the approximate "empirical" laws for the fundamental mode

$$f_0^P = f_h^P \sqrt{1 + (h/\ell)^2}$$

$$f_0^{SV} = f_h^{SV} \sqrt{1 + (2.9\ h/\ell)^2}$$

The main result of this section is that the fundamental resonance frequencies of all valleys may be satisfactorily estimated using the simple formulas given above.

Their estimation requires the knowledge of two parameters only: the one-dimensional frequency fh and the shape ratio h/l. The other parameters (Poisson ratio, impedance contrast, incidence angle) play very little role. This is, in our opinion, an important result for microzonation purposes.

Discussion

Does such a two-dimensional resonance occur in real valleys during real earthquakes?

The present numerical results have been obtained for models which are very simple as to their rheology (linear homogeneous isotropic viscoelasticity), their geometry (two-dimensional structures), and their seismic excitation (plane waves). The question then arises of their validity and applicability to real valleys in the near-field of a large earthquake.

For the rheological aspect, we may mention the experimental results of Tucker and King (1984) and King and Tucker (1984). These authors found identical spectral transfer functions over a wide acceleration range (from 10^{-5} to $0.2\,g$), which indicates that the linear is more realistic than what is usually thought in soil dynamics. Moreover, they actually observed the two-dimensional resonance in rather heterogeneous sediments, displaying a strong vertical velocity gradient. Harmsen and Harding (1981), on the other hand, have shown theoretically that sediment anisotropy has little effect on the diffraction phenomena at the interface, and therefore on the valley response.

It must be emphasized that the present results are strictly valid for two-dimensional valleys only. Such structures are nevertheless rather common (e.g., in association with river deposits), and we also think that the present results may be qualitatively extrapolated to three-dimensional circular valleys: these structures should exhibit, when deep enough, specific three-dimensional resonance patterns, among which the most simple ones to imagine are the torsional modes, and the bulk modes (see, e.g., Figures 8 and 9 of Sanchez-Sesma, 1983).

The observed independence of the resonant frequencies on the incidence angle suggests that the two-dimensional resonance modes develop whatever the incident wave field (near-field of a large earthquake, surface waves). This is further supported by the experimental results of Tucker and King (1984), who observed the same effects regardless of the source azimuth.

We thus believe that this two-dimensional resonance, or more generally a multi-dimensional resonance (two-dimensional or three-dimensional), may be expected to occur in any relatively embanked sediment-filled valley, provided that its shape ratio and velocity contrast do satisfy a condition similar to that given in Figure 12 for the two-dimensional SH case.

Application to earthquake engineering

The amplification values associated with these two-dimensional patterns are extremely large, even in the case of strong damping (Figure 8). An immediate consequence is that they must be taken into account in the assessment of the local seismic hazard. As long as empirical or theoretical relationships between amplification and valley parameters are not established, this can be done only through the use of two-dimensional models, while current practice in earthquake engineering still emphasizes the one-dimensional approach. We just want, in this section, to point out in a quantitative way the limits of such one-dimensional models.

In that aim, we considered nine sine-shaped valleys with increasing shape ratios

(from 0.05 to 1.0) and with identical mechanical parameters (velocity contrast of 5, density contrast of 1.5, and damping of 2.5 per cent). For each of them, we selected five surface sites, regularly spaced from $x/l = 0.0$ (center) to $x/l = 0.64$ (edge). We then computed, over the frequency range $[0, 4fh]$, the corresponding 9×5 SH transfer functions, from which two parameters were picked out: the frequency $fm(x)$

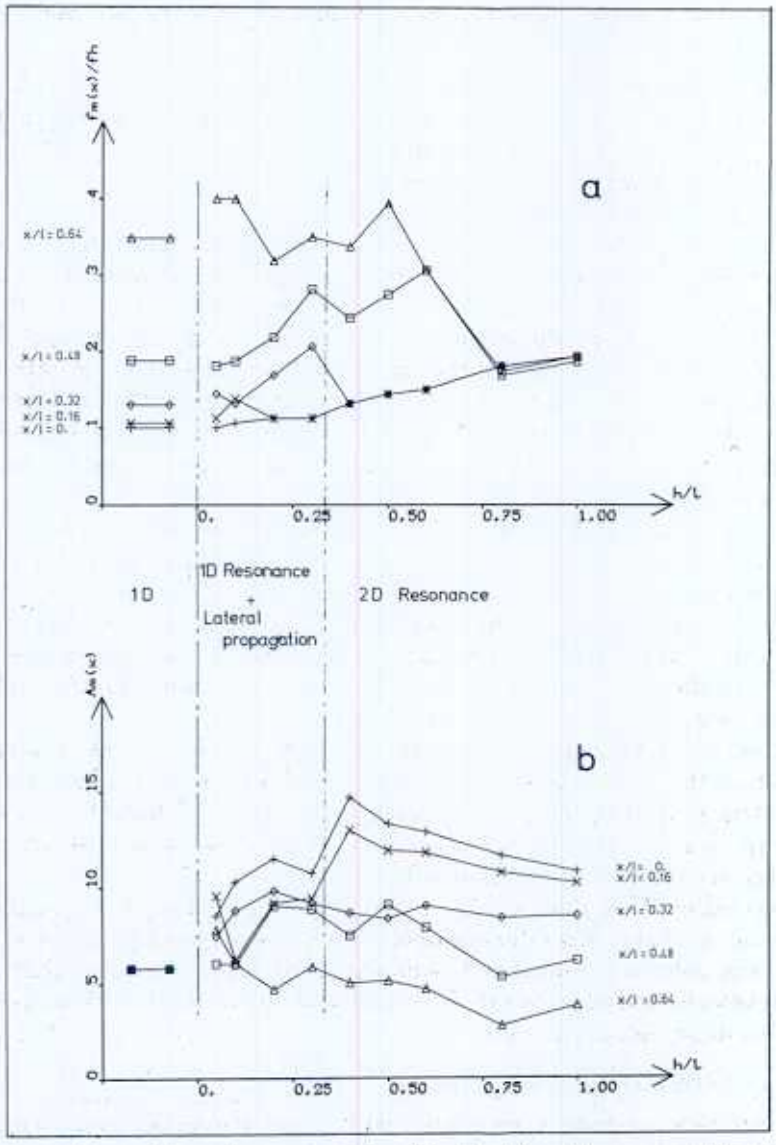

FIG. 15. Dependence of the maximum spectral amplification (b) and the corresponding frequency (a) on the shape ratio h/l for five surface sites (from $x/l = 0.$, center, to $x/l = 0.64$, edge). Both sets of results are compared with the corresponding one-dimensional (1D) values, displayed on the *left*. The geometrical and mechanical characteristics of the valleys are detailed in the text.

of the largest spectral peak, and the corresponding spectral amplitude $Am(x)$. Both quantities are displayed, respectively, in Figure 15, a and b, as a function of x/l and h/l, and compared with the corresponding one-dimensional values (which take into account only the local sediment thickness and, of course, do not depend on h/l).

Figure 15a reveals that, except for very shallow valleys ($h/l = 0.2$), the one-dimensional and two-dimensional frequencies are very different. For intermediate shape ratios, the two-dimensional frequency at $x/l = 0.32$ and $x/l = 0.48$ is significantly larger, while for large shape ratios ($h/l \geqq 0.6$), the two-dimensional frequencies are simultaneously much larger in valley center (from 40 to 80 per cent), and much smaller on the edges (less than 50 per cent at $x/l = 0.64$). As may be inferred from Figure 14, these differences would certainly be even larger if we had considered incoming SV waves. We must also mention, finally, that one-dimensional models are unable to explain the differences between the frequencies of the antiplane shear modes (SH case) and in-plane shear modes (SV case).

The divergence between one-dimensional and two-dimensional results is even larger in Figure 15b (spectral amplitudes). Despite the large damping (2.5 per cent), the two-dimensional amplification at valley center is, by far, the larger, especially around $h/l = 0.4$ (i.e., at the onset of two-dimensional resonance): the two-dimensional/one-dimensional amplitude ratio then reaches 2.5. This ratio, although lessening, remains significative (>1.5) at $x/l = 0.32$ and $x/l = 0.48$. On the opposite ratio, the two-dimensional amplitude is somewhat smaller on the edges ($x/l = 0.64$). One must remember, however, that as shown in Bouchon *et al.* (1982), the edges of sediment-filled valleys undergo very large differential motion, which cannot be predicted with one-dimensional models, and may be, as well as motion amplitude, responsible for significant damage to buildings.

This short comparison of one-dimensional and two-dimensional approaches, on the example of high-contrast sine-shaped valleys, thus shows clearly that ignoring the geometrical (two-dimensional) effects may lead to completely wrong estimates of both the amplification values and peak frequencies, even for small shape ratios. One must, therefore, be very cautious with the one-dimensional approach which, in our opinion, should be applied only in the case of almost perfectly horizontal layers.

Conclusions

We have shown on simple numerical models, the existence and the importance of specific two-dimensional mechanisms which occur in deep enough sediment-filled valleys regardless of the incident wave field.

In the present two-dimensional case, three main patterns may be distinguished, in relation with the main component of motion: the antiplane shear modes are associated with SH waves excitation; the in-plane shear modes with SV waves; and the bulk modes with P waves.

The existence conditions of this two-dimensional resonance are controlled by the valley shape ratio and by its velocity contrast. The higher the velocity contrast, the lower the "critical" shape ratio. Moreover, for a given contrast, these critical values are systematically the lowest in the SV case and the largest in the P case.

When these conditions are satisfied, the frequencies of the spectral peaks of the transfer functions are the same across the whole valley, and the corresponding phases are the same modulo 180°. These resonances thus affect the valley as a whole, and are associated with very large amplifications (up to 4 times the one-dimensional values) and with very long duration of motion.

The three fundamental modes (in-plane shear, antiplane shear, and bulk), which are the most important ones when significant damping is present, are characterized by an in-phase motion for the main component (respectively, horizontal transverse to the valley axis, horizontal parallel to the valley axis, and vertical). The corre-

sponding amplification is maximum at the valley center and regularly decreases toward the edges, where it vanishes.

The main difference between the harmonics and the fundamental is the existence of both lateral and vertical displacement nodes, on each side of which the motion is out-of-phase, and which correspond to maxima of differential motion. The largest amplifications are then located at mid-edges.

Finally, the physics of this two-dimensional resonance may be satisfactorily understood through the simple model of a soft rectangular inclusion, which moreover leads to accurate estimates of the fundamental frequencies of the three modes.

We think that all these results, although theoretical, may be regarded with confidence because of the excellent qualitative agreement between them and the most recent and detailed experimental results of Tucker and King (1984). We hope they may find practical applications in earthquake engineering and seismic microzonation studies, especially as the widely used one-dimensional approach can by no means predict the huge amplifications and frequency shifts associated with the two-dimensional geometrical effects.

ACKNOWLEDGMENTS

We thank an anonymous reviewer for his constructive comments and suggestions. Most of the calculations were made on the computer of the "Centre de Calcul Vectoriel pour la Recherche." This work was also supported by the "Institut National d'Astronomie et de Géophysique" through the ATP Sismogénèse: Plis, Failles, Mécanique de la Lithosphère.

REFERENCES

Aki, K. and K. L. Larner (1970). Surface motion of a layered medium having an irregular interface due to incident plane *SH* waves, *J. Geophys. Res.* **75**, 933–954.

Bard, P.-Y. (1983). Les effets de site d'origine structurale en sismologie, modélisation et interprétation, application au risque sismique, *Thèse d'Etat*, Université Scientifique et Médicale de Grenoble (in French), June 1983, Grenoble, France,

Bard, P.-Y. and M. Bouchon (1980a). The seismic response of sediment-filled valleys. Part I. The case of incident *SH* waves, *Bull. Seism. Soc. Am.* **70**, 1263–1286.

Bard, P.-Y. and M. Bouchon (1980b). The seismic response of sediment-filled valleys. Part II. The case of incident *P* and *SV* waves, *Bull. Seism. Soc. Am.* **70**, 1921–1941.

Bouchon, M., K. Aki, and P.-Y. Bard (1982). Theoretical evaluation of differential ground motions produced by earthquakes, *Proceedings of the 3rd International Conference on Microzonation*, Seattle, Washington, June 1982.

Harmsen, S. and S. Harding (1981). Surface motion over a sedimentary valley for incident plane *P* and *SV* waves, *Bull. Seism. Soc. Am.* **71**, 655–670.

Kagami, H., C. M. Duke, G. C. Liang, and Y. Ohta (1982). Observation of 1 to 5 second microtremors and their application to earthquake engineering. Part 2. Evaluation of site effect upon seismic wave amplification due to extremely deep soil deposits, *Bull. Seism. Soc. Am.* **72**, 987–998.

King, J. L. and B. E. Tucker (1984). Observed variations of earthquake motion over a sediment-filled valley, *Bull. Seism. Soc. Am.* **74**, 137–152.

Larner, K. L. (1970). Near receiver scattering of teleseismic body waves in layered crust-mantle models having irregular interfaces, *Ph.D. Thesis*, Massachusetts Institute of Technology, Cambridge, Massachusetts.

Sanchez-Sesma, F. J. (1983). Diffraction of elastic waves by three-dimensional surface irregularities, *Bull. Seism. Soc. Am.* **73**, 1621–1636.

Sanchez-Sesma, F. J. and J. A. Esquivel (1979). Ground motion on alluvial valleys under incident plane *SH* waves, *Bull. Seism. Soc. Am.* **69**, 1107–1120.

Trifunac, M. D. (1971). Surface motion of a semi-cylindrical alluvial valley for incident plane *SH* waves, *Bull. Seism. Soc. Am.* **61**, 1755–1770.

Tucker, B. E. and J. L. King (1984). Dependence of sediment-filled valley response on input amplitude and valley properties, *Bull. Seism. Soc. Am.* **74**, 153–166.

Wong, H. L. and M. D. Trifunac (1974). Surface motion of a semi-elliptical alluvial valley for incident plane *SH* waves, *Bull. Seism. Soc. Am.* **64**, 1389–1408.

LABORATOIRE CENTRAL DES
PONTS-ET-CHAUSSÉES
58, BOULEVARD LEFEBVRE
75732 PARIS CEDEX 15, FRANCE (P.-Y.B.)

LABORATOIRE DE GÉOPHYSIQUE INTERNE
ET DE TECTONOPHYSIQUE
ERA CNRS, No. 603
I.R.I.G.M., B.P. 68
38402 SAINT MARTIN D'HERES CEDEX,
FRANCE (P.-Y.B., M.B.)

Manuscript received 25 June 1984